

The determination of elastic modulus of slates from ultrasonic velocity measurements.

M. A. RODRÍGUEZ-SASTRE¹ & L. CALLEJA²

¹ British Geological Survey, Keyworth, Nottingham, NG12 5GG, UK. (e-mail: mrod@bgs.ac.uk)

² Universidad of Oviedo, Oviedo, Spain. (e-mail: lcalleja@geol.uniovi.es)

Abstract: Ultrasonic measurements under unconfined conditions have been measured on water-saturated slate specimen. In particular, P-wave and the S-wave velocities were studied in relation to different directions of propagation to foliation planes. As a non-destructive method of rock characterization ultrasonic methods allowed us to determine the values of dynamic elastic constants, which may be comparable to standard static elastic constants from the measurement of strain for instance using strain gauges. Ultrasonic evaluation of rock properties provides data on very small strains and provides a useful preliminary prediction of static properties.

Several blocks of slate were taken from quarries located in the Synclinal Truchas in NW Spain. Anisotropy fabrics are present in these rocks as foliation planes. Rock samples were orientated with respect to the foliation and stratification planes. Different orientations of the main anisotropy planes were obtained during the specimen preparation. Variations of velocities were recorded and correlated with the foliation planes. The dynamic elastic constants of slates were calculated using standard formulae and their anisotropy determined and the results are presented.

Résumé: Les mesures ultrasoniques sous les conditions non-confinées ont été mesurées sur des spécimens eau-saturés d'ardoise. En particulier, la vitesse des ondes P et S a été étudiée en relation avec différentes directions de la propagation aux planes de foliation. Bien que l'essai ultrasonique soit une méthode non destructive de caractérisation de roche il a un inconvénient que les valeurs des constantes élastiques qui sont obtenues souvent plus hautes que ceux déterminées par des méthodes statiques de laboratoire. L'évaluation ultrasonique des propriétés de roche est néanmoins une prévision préliminaire utile des propriétés statiques. Plusieurs blocs d'ardoise ont été pris des carrières situées dans le Synclinal Truchas au Nord-Ouest d'Espagne. Les planes d'anisotropie sont présents dans ces roches comme planes de foliation. Des échantillons de roche ont été orientés en ce qui concerne les planes de foliation et de stratification. Différentes orientations des plans principaux d'anisotropie ont été obtenues pendant la préparation de spécimens. Des variations des vitesses ont été enregistrées et corrélées avec les planes de foliation. Les constantes élastiques des ardoises étaient déterminées en utilisant les équations d'ASTM.

Keywords: metamorphic rocks, laboratory test, rock mechanics, quarries, geophysics and saturated materials

INTRODUCTION

The elastic moduli of rocks are normally evaluated in the laboratory using a conventional uniaxial compressive test often with strain gauges stuck on cylindrical samples. However, the use of ultrasonic testing to determine pulse velocities and the calculation of dynamic elastic constants for rocks are in ASTM (1995) procedures, standard D2845-95. It was applied on rocks from the Truchas Syncline area (NW of Spain) where important engineering works have been developed in the last century. The issue of this study was to establish the elastic modulus required for the design and construction of foundations, in tunnelling and in slope stability studies. Ultrasonic methods have also been used as a non-destructive method, which can inform about the behaviour of these mass rocks during exploitation works in slates (McCann & Fenning, 1995).

In order to determine a proper understanding of these rocks a petrography study from naked eye to microscopic observations have been carried on. The measurements of physical properties in slates have also been determined (Rodríguez-Sastre, 2003). Metamorphic rocks are mainly characterized by the presence of anisotropy planes known as foliation, which are planes of weakness, and were developed during the metamorphic phases. Those planes have been developed due to the alignment of minerals during the metamorphic deformation under low-grade conditions (Chlorite zone). Little information about anisotropy influence upon elastic modules is available for metamorphic rocks. However, it is well known that elastic wave propagation is very sensitive to anisotropies so velocities propagating along the oriented fractures are characterized by being higher than across them (Ivankina, Dern and Nikitin, 2005).

This paper presents the determination of ultrasonic velocity (P-wave and S-wave) for saturated and unweathered cores and decimetre rectangular rock specimens. Velocities were measured to determine the influence of the foliation planes in the elastic modulus under unconfined conditions. The principal variations of the wave propagation in relation with anisotropy planes were recorded as well as the variations on the three kinds of samples with slightly different lithology.

METHOD

Rock properties, including ultrasonic velocities, were measured in samples collected from quarry outcrops that were sited on each limb of the Syncline Truchas; samples from Casaio Formation on the southern limb, and Rozadais Formation on the northern limb. Three slate types were selected for the present study: fine grain slate, silty slate and slate with millimetre sandstone laminations (Figure 1).

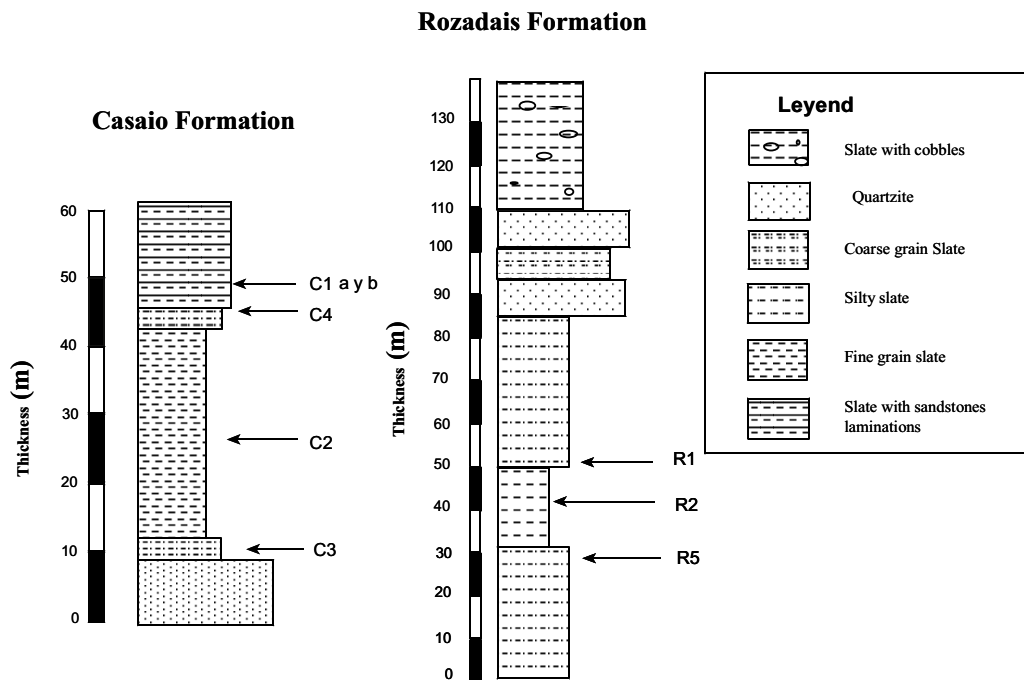


Figure 1. Lithological sequences where samples were taken in slates of Truchas Syncline

Unweathered rock samples were obtained from a hundred quarry blocks and cut parallel and perpendicular to foliation plane and on XZ and YZ planes with different sets of angles for the foliation planes (Figure 2). In this study, therefore, different inclination of anisotropy planes was established by the definition of β angle ($\beta=0^\circ$ corresponds to properties at right angles to the foliation plane and $\beta=90^\circ$ correspond to properties along the foliation plane, and another samples were drilled at β angles of 15, 35, 45 and 60°). From the selected blocks, test cores were drilled 54 mm diameter (NX cores) and rectangular rocks were manufactured to determine physical rock properties and wave velocities. Consequently, the axes of the cubes were parallel and normal to foliation (XY plane). During sample preparation and until the moment of the test, specimens were water saturated throughout. It was important to establish, in each rock sample and when ever possible, the relation between foliation and bending planes. It could easily be recorded in the case of slates with sandstone laminations whilst in the rest of lithologies stratification planes were not well developed.

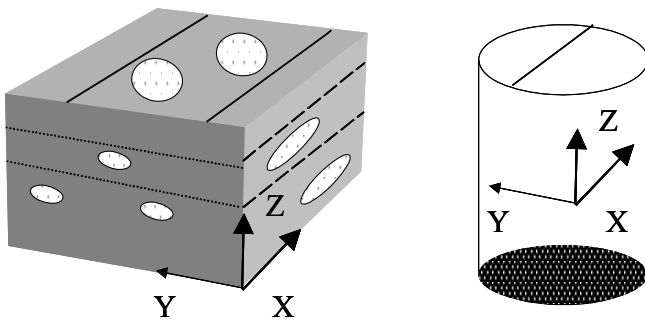


Figure 2. Rock block lineation and sample orientation in slates of Truchas Syncline.

The laboratory velocity measurements were done using ultrasonic equipment (OYO Cop. Mod. 5.217). Transmitting and receiving transducers were mounted at the opposing ends of the samples (P-wave transducers 45 kHz frequency and S-wave transducers 33 kHz frequency). P-wave and S-wave measurements were made on all the cores in longitudinal mode (Z direction), and in the rectangular rock in the three orthogonal directions. Consequently, the samples are tested with reference to the foliation and lineation (Z is normal to foliation, Y perpendicular to lineation within the foliation and X parallel to lineation). The travel time required for the wave to reach from one end to the other end of the sample is measured. The shear and compression wave velocities are calculated by dividing the length of travelling by the time taken to travel the distance between the transducer faces.

Samples were kept under water saturation conditions, and measurements were recorded at room pressure and temperature after 36 hours in immersion water. A total of 93 measurements were taken on samples with different foliation disposition defined as β angle. NX-core samples diameters varied from 53.26 and 54.22 mm and the lengths ranged between 36 and 176 mm.

The compression and shear wave velocities, V_p and V_s are used to calculate the dynamic elastic constants with the standard equations as presented in ASTM (1995).

$$E = \frac{[\rho \times V_s^2 \times (3 \times V_p^2 - 4 \times V_s^2)]}{(V_p^2 - V_s^2)}$$

$$G = \rho \times V_s^2$$

$$\nu = \frac{(V_p^2 - 2 \times V_s^2)}{[2 \times (V_p^2 - V_s^2)]}$$

$$\lambda = \rho \times (V_p^2 - 2 \times V_s^2)$$

$$K = \frac{\rho \times (3 \times V_p^2 - 4 \times V_s^2)}{3}$$

where E is Young's Modulus, G is Modulus of rigidity or shear modulus, ν is Poisson's ratio, λ is Lamé's constant, and K is Bulk modulus. V_p and V_s are compression and shear waves velocities and ρ is density.

Although values of elastic constants properties tend to be higher than those preliminary predicted by static laboratory methods ultrasonic evaluation of rock properties these values are nonetheless a useful preliminary prediction of static properties (Calleja, 1985; Sharma, 1986; Alonso, 1986; Entwisle & McCann, 1990; Jonson & Degraff, 1994; Hassani, Sadri & Momayez, 1997; Dobrin & Savit, 1988; González de Vallejo et al., 2002, Turcotte, 2002, Blyth & de Freitas, 2003).

RESULTS AND DISCUSSION

Petrography

The three lithologies from the Casaio Formation ('C' samples) selected were fine grain slate, silty slate and slate with sandstone interlayered laminations, and from the Rozadais Formation ('R' samples) fine grain and silty slates were used.

Thin sections were used to study the mineralogy and metamorphic textures to obtain a full insight into the composition and genesis of these rocks determine the variation of those features in orthogonal sections. Microscopic descriptions of fine grain slates (C2 and R2 in a XY and YZ section respectively) show lepidoblastic and layered lattice textures. In the Casaio Formation samples the average grain size of chlorite blasts is <0.3 mm of chlorites blast, which are surrounded by fine grain chlorite, quartz and muscovite of <0.1mm. In the Rozadais Formation samples the most abundant minerals are muscovite, quartz, chlorite surrounding postcinematic opaque minerals. The main microstructure is slaty foliation in slate domains while in quartz grain zones a rough foliation has been established.

The C1 sample is a grey slate with foliation planes and quartz-rich zones interlayered with 3-5 cm thick. Those zones reflect the original sedimentary layers. However, two different lithological types were identified that had different relationships between the sandstone lamination and foliation planes. Subtype C1a, had sub parallel sandstone laminations, with 20° inclination respect to the foliation surfaces. Subtype C1b was a slate with sandstone laminations being nearly orthogonal to the foliation planes. Otherwise, 'a' type is more uniform than 'b' type, which also had a better facility to split than the 'a' type slate.

C2 sample is a fine grain slate with abundant sulphur minerals of millimetre size concentrated mainly on foliation surfaces. C3 sample is a silty slate characterized by 1-2 cm nodules, which consist of quartz and sulphurous minerals mainly; quartz-rich zones have been observed. C4 sample consist of a uniform grey silty slate.

Sample R1 is a grey bluish slate with a bimodal size of iron sulphide, which varies from millimetre to centimetre in size. R2 sample is a grey bluish slate with millimetre widespread sulphurs, R5 being a silty slate bluish with a some sulphur minerals.

Physical properties

Fundamental rock properties have been determined for these slates. The tests include moisture content, dry and bulk density using methods described in UNE (AENOR, 1999) and ASTM (1982) (Spanish and American test standards respectively). A total of 36 cylindrical samples were used for the basic rock properties (in sets of five with same lithologic composition for each formation studied), and 62 were used to determine moisture content.

The main basic physical properties determined were: moisture content, index of pores, free water absorption, and bulk densities. The data are summarized in Table 2. Density values for Rozadais slates (R1, R2 and R5) shows that fine grain rocks are slightly denser, whereas, those samples with greater quartz content are slightly less dense (2.79 g/cm^3 in slates with sandy laminations). In general, the densities of both formations were similar.

Velocity measurements

In this section results obtained from the measurement of velocities are analyzed (Table 2). The P-wave velocities range from 2,691 to 6,743 m/s and for S-wave velocity varied between 1,196 and 4,769 m/s.

Average data obtained from rectangular rock samples along the three orthogonal directions are summarized in Table 3, in order to examine the influence of rock microstructure. P-wave velocities vary between 2,691 and 6,991 m/s and S-wave velocities between 1,172 and 3,482 m/s. XY direction velocities have lower values than those obtained in the other directions XZ and YZ. This is due to foliation planes with slight undulations and being not perfectly straight, although there could be interferences from the rich-quartz zones present in these rocks.

Table 1. Rock physical properties for slates from Truchas Syncline.

| Physical parameters | Formation | |
|------------------------------------|-----------|-----------|
| | Casaio | Rozadais |
| Natural Moisture content (%) | <0.004 | 0.00 |
| Saturation of moisture content (%) | 0.07-0.35 | 0.12-0.15 |
| Void Index, I_v (%) | 0.03-0.08 | - |
| Free water absorption (%) | <0.07 | 0,03 |
| Bulk density (g/cm^3) | 2.47-2.76 | 2.73-2.89 |
| Porosity (%) | <0.01 | <0.004 |

Table 2. P- and S-wave velocities results on specimens from Truchas Syncline.

| Formation | Sample* | Specimen shape | β (°) | Average V_p (m/s) | Average V_s (m/s) | V_p/V_s |
|-----------|----------|----------------------------|-------------|---------------------|---------------------|-----------|
| Rozadais | R2 (4) | NX Core | 0 | 3,989 | 1,899 | 2.10 |
| | R2 (4) † | NX Core | 30 | 4,601 | 2,228 | 2.06 |
| | R1 (3) | NX Core | 0 | 4,729 | 2,489 | 1.90 |
| | R1 | NX Core | 90 | 6,154 | 3,385 | 1.82 |
| | R2 (2) | NX Core | 90 | 6,362 | 4,769 | 1.33 |
| | R5(5) | Rectangular rock | 0 | 3,788 | 1,317 | 2.88 |
| | R5(2) † | NX Core | 30 | 4,922 | 2,455 | 2.00 |
| | R5 (10) | Rectangular rock | 90 | 5,756 | 2,845 | 2.02 |
| Casaio | C4(4) | NX Core | 10 | 3,250 | 1,774 | 1.83 |
| | C4 | NX Core | 45 | 4,361 | 2,181 | 2.00 |
| | C4 | NX Core | 60 | 4,759 | 2,826 | 1.68 |
| | C4(2) | Rectangular rock | 90 | 5,894 | 2,973 | 1.98 |
| | C4 | Rectangular rock | 0 | 2,691 | 1,473 | 1.83 |
| | C4 | NX Core | 25 | 4,352 | 2,210 | 1.97 |
| | C2 | NX Core + Rectangular rock | 90 | 6,743 | 3,126 | 2.16 |
| | C2 | NX Core | 60 | 5,333 | 2,783 | 1.92 |
| | C2 (3) | NX Core | 35 | 4,692 | 2,499 | 1.88 |
| | C2 (2) | NX Core | 25 | 4,190 | 2,414 | 1.74 |
| | C2 (7) | NX Core | 45 | 4,551 | 2,423 | 1.88 |
| | C2 | NX Core + Rectangular rock | 0 | 3,743 | 1,860 | 2.01 |
| | C3 (2) | NX Core | 60 | 5,386 | 2,695 | 2.00 |
| | C3 | NX Core | 25 | 4,241 | 2,121 | 2.00 |
| | C3 | NX Core | 35 | 4,377 | 2,278 | 1.92 |
| | C3 (4) | NX Core | 45 | 4,557 | 2,131 | 2.14 |
| | C1a | NX Core | 90 | 6,539 | 3,062 | 2.14 |
| | C1a (2) | NX Core | 60 | 5,100 | 2,336 | 2.18 |
| | C1a | NX Core | 45 | 4,453 | 2,284 | 1.95 |
| | C1a (3) | NX Core | 35 | 4,354 | 2,310 | 1.88 |
| | C1a (4) | NX Core | 25 | 4,125 | 2,301 | 1.79 |
| | C1a (6) | NX Core + Rectangular rock | 0 | 4,057 | 2,284 | 1.78 |
| | C1b | NX Core + Rectangular rock | 0 | 3,577 | 1,873 | 1.91 |
| | C1b | NX Core | 10 | 3,546 | 1,196 | 2.96 |
| C1b (3) | NX Core | 35 | 4,465 | 2,408 | 1.85 | |
| C1b | NX Core | 90 | 5,989 | 2,974 | 2.01 | |

* Number in bracket means the number of samples measured in each test and in the rest of the case are the unite

† Data CEDEX report, 1998

V_p and V_s taken in XY direction, show that the highest values in the slates with sandstone laminations and it had not been found any relation with the other directions measured. V_p value for both formations are much lower in the XY direction ($\beta = 0^\circ$) than in the XZ and YZ directions ($\beta = 90^\circ$).

Table 3. Summary of velocities measured in three orthogonal directions in rectangular rock samples.

| Formation | Sample | V_p (m/s) | | | V_s (m/s) | | |
|-----------|--------|-------------|-------|-------|-------------|-------|-------|
| | | (XY) | (XZ) | (YZ) | (XY) | (XZ) | (YZ) |
| Casaio | C2-M | 3,186 | 6,437 | 6,848 | 1,172 | 3,061 | 3,482 |
| | C4 | 2,691 | 5,711 | 6,078 | 1,473 | 2,786 | 3,161 |
| | C1b | 3,936 | 5,816 | 6,162 | 2,019 | 2,908 | 3,040 |
| | C1a | 3,666 | 6,442 | 6,636 | 1,990 | 3,221 | 2,903 |
| | C2 | 3,327 | 6,504 | 6,991 | 1,683 | 3,136 | 3,263 |
| Rozadais | R5 | 3,788 | 5,813 | 5,699 | 1,317 | 2,927 | 2,763 |

An equation to show relation between velocities and different orientations is given below. This indicates the influence of anisotropy along the foliation planes and how the quartz-rich zones, seen under microscope, could influence velocity of wave propagation. Anisotropy index, I_a , was calculated using the following equation:

$$Ia_v = \frac{V_{xz} + V_{yz}}{2 \times V_{xy}}$$

The coefficient of velocity anisotropy, Ia_v , varies between 1.33 and 2.19, which means low-medium anisotropies index for these rocks, following Ramamurphy (1993) classifications. Otherwise, following Ivankina et al. (2005), coefficients of velocity anisotropy can be defined as:

$$A = \left(\frac{V_{\max} - V_{\min}}{V_{\text{average}}} \right) \times 100\%$$

In that case, the main factor producing velocity anisotropy is the different lithological composition of the rock materials (Figure 3). Anisotropy index calculated ranges from 34.47% to 70.17% for P-wave measurements and 33.76% to 89.83% for S-wave velocity. It is important to note that high quartz content means lower anisotropy index, which is best shown by S-waves velocity. Consequently, the relative proportions of major minerals, their elastic properties, and their orientations control velocity anisotropy in anisotropy rocks.

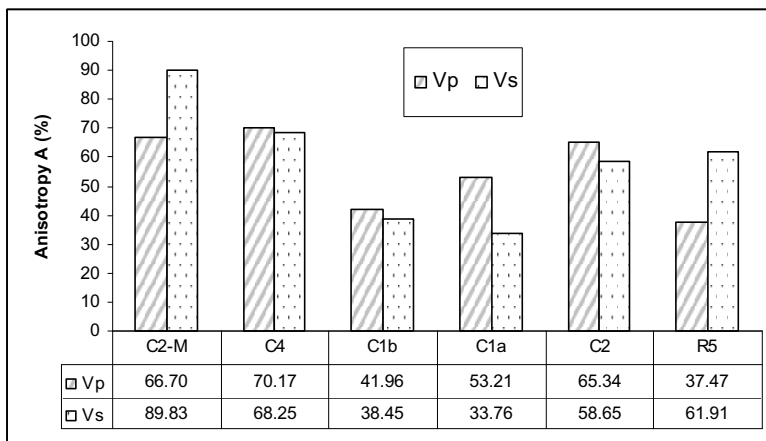


Figure 3. Anisotropy index calculated for Truchas Syncline samples.

In general, mainly for core sample test results, the maximum values are for an angle β of 90° and minimum at 0° . Correlations between velocities and β angle are linear and the correlation coefficients are good to very good. These correlations are higher in the case of P-waves than S-waves; however, samples C2 and C4 had the highest velocity values. This is due to the influence of foliation planes and the lithological composition on the wave transmission.

Elastic constants

Applying elastic constant equations, mainly for core samples and some rectangular block samples, dynamic elastic moduli were calculated in slates and these results are summarized in Table 4.

The density values used in the calculations were 2.82 Mg/m^3 for R2 and C2, 2.81 Mg/m^3 for R1, R5, C3 and C4, and 2.76 Mg/m^3 for C1a and C1b. In order to study the influence of foliation plane angle in samples, mean values of elastic modulus were plotted against dip angle.

A strong correlation between Young's modulus and anisotropy angle, between 0.6 and 0.9, indicates that velocities increase with higher inclination of foliation planes (Figure 4). In general, the maximum values of the constants, except Poisson's ratio, are for a β of 90° and minimum values for β of 0° and no clear dependence on the type of slate lithological. From those results it is important to note that foliation has an important control on elastic constants.

It seems that, in general, anisotropy does affect all the dynamic elastic constants, Poisson's ratio having the smallest relative change, with the exclusion of C1a samples (Figures. 5, 6, 7 & 8). The highest values of dynamic elastic moduli are for foliation dip angles of 90° and the lowest values are for foliation dip angles of 0° .

The orientation of foliation for the cube samples also affects the values of dynamic elastic moduli. Minimum values were obtained in Z-axis direction, maximum values for the X direction and the Y direction had intermediate values. It is thought that the lower values for the Z direction is due to the foliation anisotropy, whereas in the values for the X and Y direction are influenced by the mineral orientation.

Table 4. Summary of elastic modulus for slates from Truchas Syncline.

| Formation | Sample | $\beta(^{\circ})$ | Ex10 ⁴ (MPa) | | | ν (-) | | | G x10 ⁴ (MPa) | Kx10 ⁴ (MPa) | λ x 10 ⁴ (MPa) |
|-----------|---------|-------------------|-------------------------|------|-------|-----------|-------|-------|-----------------------------|-------------------------|--------------------------------------|
| | | | Max. | Min. | Aver. | Max. | Min. | Aver. | Aver. | Aver. | Aver. |
| Rozadais | R2 (4) | 0 | 3.10 | 2.30 | 2.76 | 0.39 | 0.32 | 0.35 | 1.02 | 3.14 | 3.48 |
| | R1 (3) | 0 | 5.54 | 3.79 | 4.58 | 0.33 | 0.29 | 0.31 | 1.64 | 3.66 | 4.21 |
| | R5(5) | 0 | 1.95 | 0.97 | 1.40 | 0.46 | 0.34 | 0.42 | 0.49 | 3.48 | 3.65 |
| | R1 | 90 | - | - | 8.25 | - | - | 0.31 | 2.43 | 4.79 | 5.60 |
| | R2 (2) | 90 | 12.28 | 8.87 | 10.58 | -0.02 | -0.33 | -0.17 | 6.42 | 2.88 | 5.02 |
| | R5 (10) | 90 | 7.04 | 4.57 | 6.11 | 0.36 | 0.32 | 0.34 | 2.36 | 6.39 | 7.18 |
| Casaio | C4(4) | 10 | 2.80 | 1.54 | 2.23 | 0.38 | 0.14 | 0.26 | 0.91 | 1.76 | 2.06 |
| | C4 | 45 | - | - | 3.56 | - | - | 0.33 | 1.34 | 3.56 | 4.01 |
| | C4 | 60 | - | - | 5.51 | - | - | 0.23 | 2.24 | 3.37 | 4.12 |
| | C4 | 0 | - | - | 1.57 | - | - | 0.28 | 0.61 | 1.22 | 1.42 |
| | C4(2) | 90 | 7.38 | 5.86 | 6.62 | 0.34 | 0.31 | 0.33 | 1.86 | 5.07 | 5.69 |
| | C4 | 25 | - | - | 3.66 | - | - | 0.32 | 1.38 | 3.48 | 3.94 |
| | C2 | 90 | - | - | 7.49 | - | - | 0.36 | 2.76 | 9.15 | 10.07 |
| | C2 | 60 | - | - | 5.71 | - | - | 0.31 | 2.18 | 5.11 | 5.84 |
| | C2 (4) | 35 | 4.38 | 2.83 | 3.65 | 0.36 | 0.21 | 0.28 | 1.77 | 3.86 | 4.44 |
| | C2 (2) | 25 | 4.42 | 3.82 | 4.12 | 0.26 | 0.24 | 0.25 | 1.65 | 2.76 | 3.31 |
| | C2 (7) | 45 | 5.54 | 3.20 | 4.31 | 0.37 | 0.20 | 0.29 | 1.68 | 3.60 | 4.16 |
| | C2 | 0 | - | - | 2.61 | - | - | 0.34 | 0.98 | 2.65 | 2.98 |
| | C3 (2) | 60 | 5.58 | 5.29 | 5.43 | 0.35 | 0.31 | 0.33 | 2.04 | 5.45 | 6.13 |
| | C3 | 25 | - | - | 3.37 | - | - | 0.33 | 1.26 | 3.37 | 3.79 |
| | C3 | 35 | - | - | 3.83 | - | - | 0.31 | 1.46 | 3.44 | 3.93 |
| | C3 (4) | 45 | 4.36 | 3.00 | 3.44 | 0.40 | 0.34 | 0.29 | 1.29 | 3.88 | 4.31 |
| | C1a (2) | 90 | 7.64 | 6.43 | 7.03 | 0.38 | 0.33 | 0.36 | 2.54 | 7.04 | 8.24 |
| | C1a (2) | 60 | 4.20 | 4.03 | 4.12 | 0.37 | 0.36 | 0.37 | 1.51 | 5.17 | 5.68 |
| | C1a | 45 | - | - | 3.80 | - | - | 0.32 | 1.44 | 3.55 | 4.03 |
| | C1a (3) | 35 | 4.24 | 3.51 | 3.76 | 0.35 | 0.16 | 0.28 | 1.48 | 3.27 | 3.76 |
| | C1a (4) | 25 | 4.45 | 3.16 | 3.70 | 0.34 | 0.18 | 0.27 | 1.47 | 2.74 | 3.23 |
| | C1a (6) | 0 | 4.16 | 2.71 | 3.66 | 0.31 | 0.21 | 0.27 | 1.45 | 2.64 | 3.12 |
| | C1b | 0 | - | - | 2.54 | - | - | 0.31 | 0.97 | 2.24 | 2.56 |
| | C1b | 10 | - | - | 1.13 | - | - | 0.44 | 0.39 | 2.94 | 3.08 |
| | C1b (3) | 35 | 4.57 | 4.00 | 4.19 | 0.33 | 0.26 | 0.29 | 1.60 | 3.37 | 3.91 |
| | C1b | 90 | 6.70 | 6.29 | 6.50 | 0.38 | 0.31 | 0.33 | 2.42 | 7.96 | 7.96 |

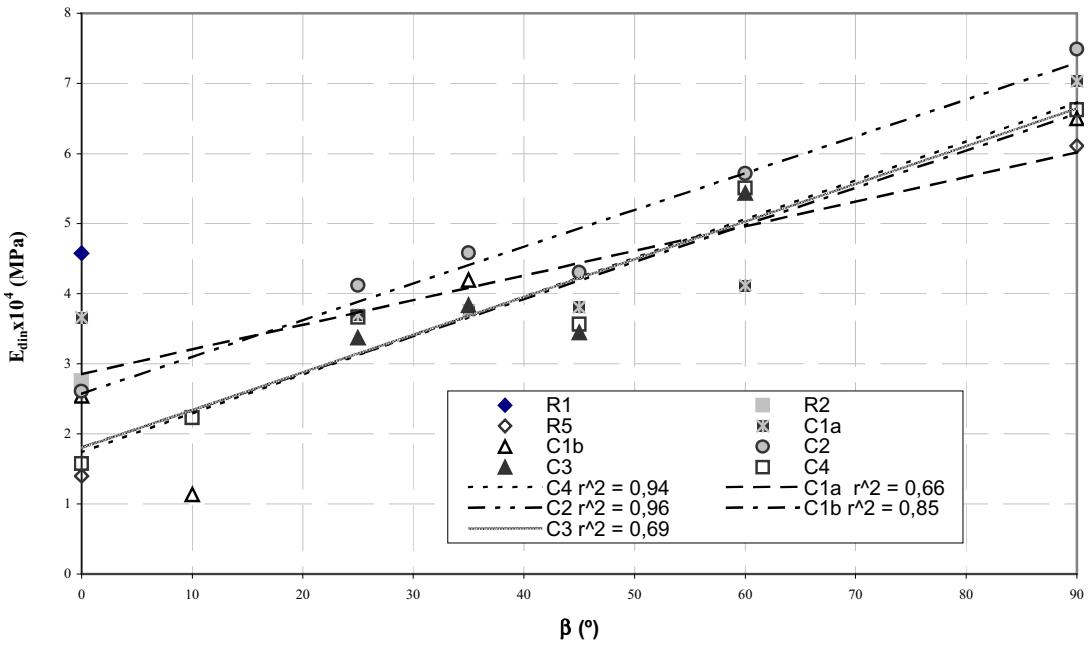


Figure 4. Correlation Young's Modulus with foliation dip angle for slates specimens.

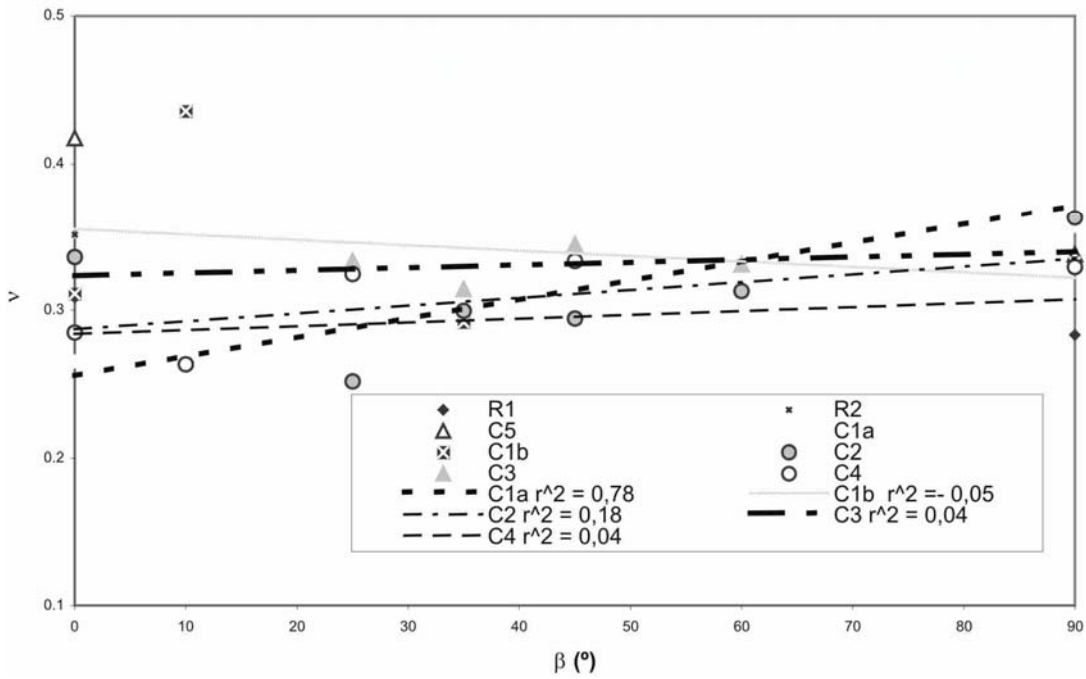


Figure 5. Correlation Poisson ratio with foliation dip angle for slates specimens.

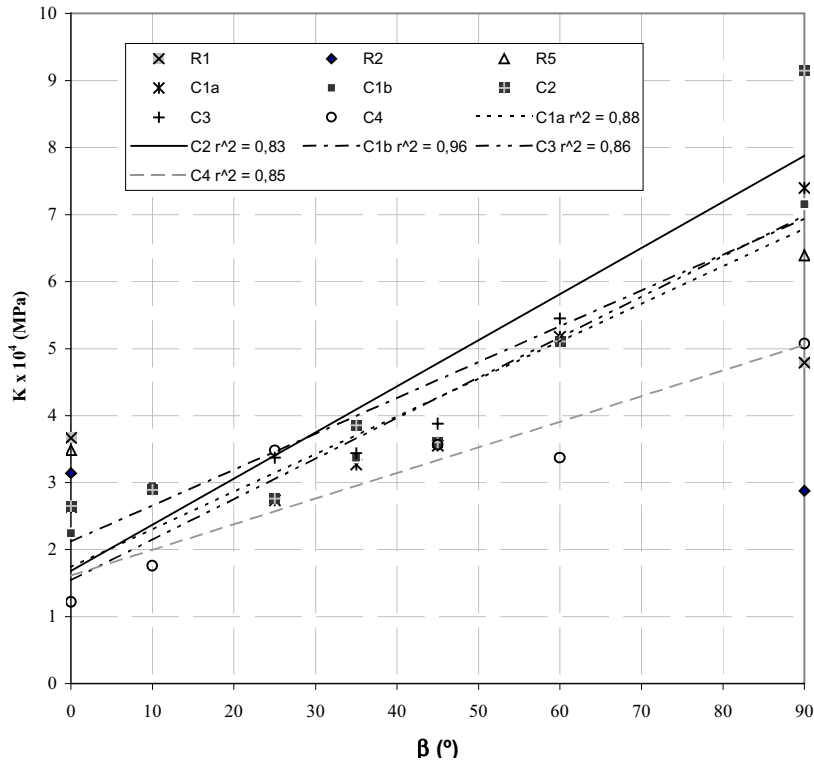


Figure 6. Correlation Bulk modulus with foliation dip angle for slates specimens.

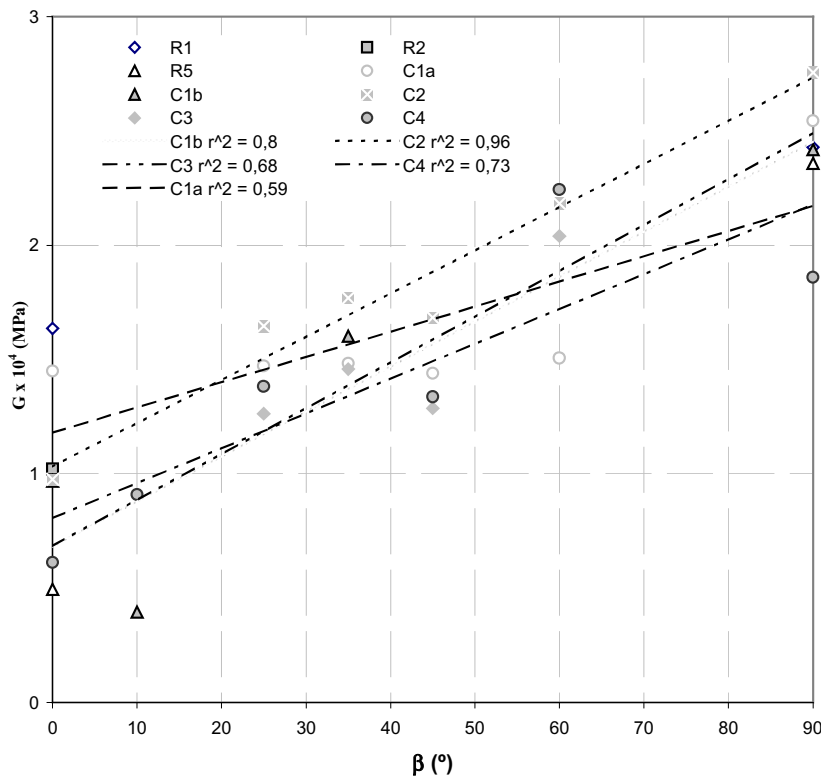


Figure 7. Correlation Shear modulus with foliation dip angle for slates specimens.

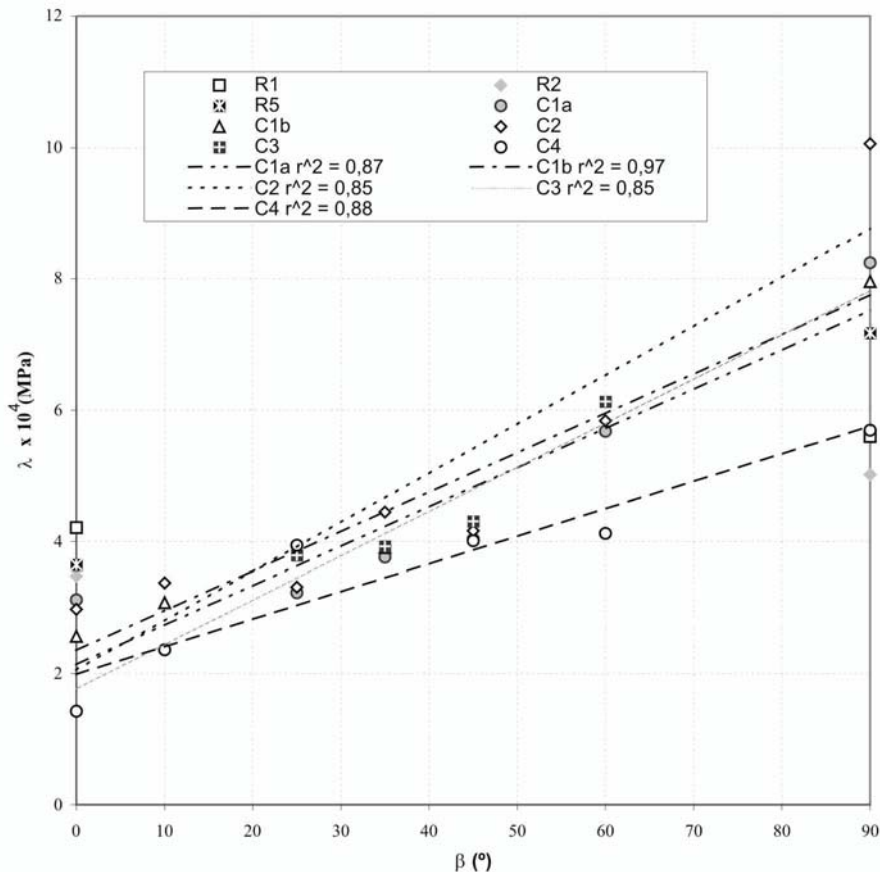


Figure 8. Correlation Lamé's constant with foliation dip angle for slates specimens

CONCLUSIONS

Under unconfined conditions, the propagation of ultrasonic wave through the slate rocks from the Truchas Syncline is partly controlled by the foliation planes.

Maximum ultrasonic wave velocities and dynamic elastic moduli correspond with a foliation inclination of 90°, where the wave propagation is parallel to such orientation, and the lowest values were for a foliation inclination of 0°. The data show a good linear correlation between the increase in the inclination angle of the foliation and the dynamic elastic constants (E, K, G and λ), but this is less marked for Poisson Modulus (ν).

During engineering works on slate outcrops, a careful analysis of anisotropy and lineation on rocks will be required. Ultrasonic methods, carried out at different orientations in relation to the foliation, may be used to show the degree of anisotropy and those planes with lower dynamic elastic moduli.

Acknowledgements: Authors acknowledge a post-doctoral grant from the Spanish Ministerio de Educación, Cultura y deporte held at the British Geological Survey. Thanks to Dr. C. Evans and Dr Efthimios Tartaras for help greatly in improving the manuscript. Field and laboratory expenses were funded from research project FEDER ID97-0959-C03.

Corresponding author: Dr M. A. Rodríguez-Sastre. BGS. Nicker Hill. Keyworth. Notts. NG12 5GG. United Kingdom. Tel: +44 1159363292. Email: mrod@bgs.ac.uk.

REFERENCES

- AENOR. 1999. *Geotecnia. Ensayos de campo y de laboratorio*. Asociación Española de Normalización y Certificación, Madrid. (in Spanish).
- ALONSO F.J. 1986. *Caracterización petrofísica y alterabilidad de calizas y dolomías*. Thesis, University of Oviedo. (in Spanish).
- ASTM. 1995. *Standard test method for laboratory determination of pulse velocities and ultrasonics elastic constants of rocks, D. 2845-95. Annual Book of A.S.T.M. Standards, 4.08*. American Society for Testing and Materials, West Conshocken, PA.
- BLYTH, F. G. H. & DE FREITAS, M.H. 2003. *A geology for Engineers*. 7th Edition. Butterworth-Heinemann, Great Britain.
- CALLEJA, L. 1985. *Variación de propiedades físicas en rocas cristalinas sometidas a gradientes térmicos*. Thesis, University of Oviedo. (in Spanish).
- CEDEX. 1998. Resultados de los ensayos realizados con muestras de pizarras procedentes de Puente Domingo Flórez (León). Report for Pizarras Expiz. (in Spanish).

- DOBRIN, B.M. & SAVIT, C.H. 1988. *Introduction to geophysical prospecting*. 4th Edition. Ed. McGraw-Hill.
- ENTWISLE, D. C. & McCANN, D. M. 1990. An assessment of the use of Christensen's equation for the prediction of shear wave velocity and engineering parameters. In: *Geological Applications of Wireline Logs. Geological Society Special Publication No. 48*: Geological Society of London. London. 347-354.
- GONZÁLEZ DE VALLEJO, L.I., FERRER, M., ORTUÑO, L. & OTEO, C. 2002. *Ingeniería Geológica*. Ed. Pearson Education, Madrid. (in Spanish).
- HASSANI, P.P., SADRI, A. & MOMAYEZ, M. 1997. A miniature seismic reflection system for evaluation of concrete Linings. *Pure and Applied geophysics*. **10**: 677-691.
- IVANKINA T.I., DERN, K.M. & NIKITIN, A.N., 2005. Directional dependence of P and S wave propagation and polarization in foliated rocks from the Kola superdeep well: Evidence from laboratory measurements and calculations based on TOF neutron diffraction. *Tectonophysics* **407**, 25-42.
- JONSON, R.B. & DEGRAFF, J.V. 1994. *Engineering Geology*. Ed. Macmillan.
- MCANN, D.M. & FENNING, P.J. 1995. Estimation of rippability and excavation conditions from seismic velocity measurements. In: *Engineering Geology of Construction. The Geological Society, London. Engineering Geology Special Publication 10*: 335-343.
- RAMAMURPHY, T. 1993. Strength and Modulus Responses of Anisotropic Rocks. In: *Comprehensive Rock Engineering, Principles, Practice and Projects*. **3**, 313-329.
- RODRÍGUEZ SASTRE, M.A. 2003. *Caracterización geomecánica de materiales pizarrosos del Sinclinal de Truchas (León-Orense)*. Thesis, University of Oviedo. (in Spanish).
- SHARMA, P.V. 1986. *Geophysical Methods in geology*. 2nd Edition Ed. Elsevier, Amsterdam.
- TURCOTTE, D.L. & SCHUBERT, G. 2002. *Geodynamics*. 2nd Edition. University Press, Cambridge.